Regional Geology and Resource Potential of the Chezacut Map Area, Central British Columbia (NTS 093C/08)

by M.G. Mihalynuk, C.R. Peat, K. Terhune and E.A. Orovan[1]

KEYWORDS: regional geology, structure, lithogeochemistry, mineral potential, Chezacut, Chilcotin River, mountain pine beetle

INTRODUCTION

Mountain pine beetles are a natural part of western North American forest ecosystems. They range from British Columbia to northern Mexico. Human intervention in the natural cycle of forest fires, which rejuvenate forests and create barriers to the transmission of disease and pests, has resulted in mature to overmature pine forests throughout interior British Columbia. These stands of trees are particularly susceptible to widespread mountain pine beetle infestation. A combination of enhanced beetle survival during recent mild winters and regionally overmature forests has resulted in a beetle-infested area of historically unprecedented size. In 2005, the area of contiguous infestation recorded by the *2004 Forest Health Survey* (BC Ministry of Forests and Range, 2005a) was coextensive with the Interior Plateau (Fig 1). We refer to this area as the Beetle Infested Zone (BIZ; Mihalynuk*,* 2007).

Substantial increases to the annual allowable timber harvest in most of the BIZ will help to capture economic value from the dead trees, speed up regeneration and enhance economies of forestry-dependent communities in the BIZ (BC Ministry of Forests and Range, 2005b). However, inevitable degradation of the available trees will lead to an industry downturn. The provincial government is supporting economic diversification to help reduce the long-term economic impact of the mountain pine beetle, including geological mapping programs aimed at locating areas of potential interest to the mining and petroleum industries.

The Chezacut area was targeted for revision mapping because of relatively good logging road access and a historical lack of mineral exploration that we believe is undeserved. Herein we report on results of geological mapping and resource evaluation of the area in the 2007 field season and confirm that further mineral exploration is warranted. Significant mineralization was discovered within the first two weeks of mapping (*see* 'Mineralization' section). Geological mapping also demonstrated that rock exposures are more extensive, and Chilcotin basalt is less extensive, than previously recognized — additional incentives for future mineral exploration in the area.

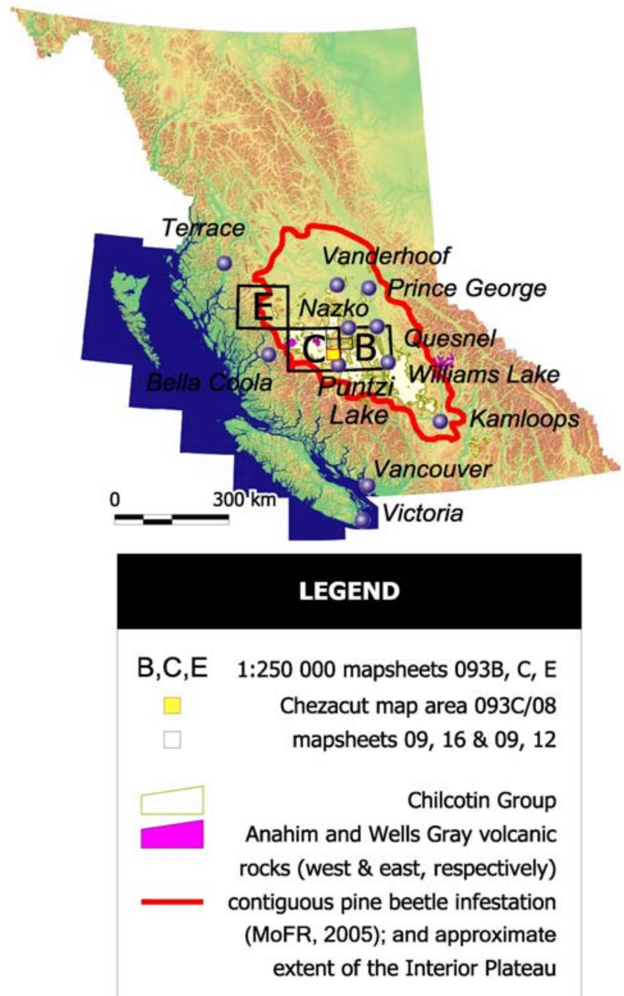

Figure 1. Location of the Chezacut map area, showing areas mentioned in the text as well as the distribution of rocks of the Chilcotin Group (*after* Massey et al., 2005).

LOCATION AND ACCESS

The map area covers approximately 950 km^2, and is located about 200 km west of Williams Lake on the Fraser Plateau (the Interior Plateau, Fig 1). It is immediately north of the resort community of Puntzi Lake, a former military air base on the north side of Highway 20 approximately halfway between Williams Lake and Bella Coola. Midway along the eastern edge of the map area is the tiny ranching community of Chezacut, serviced from the main Chezacut forest service road. A second major forest service road, the

[1] *Carleton University, Ottawa, ON*

This publication is also available, free of charge, as colour digital files in Adobe Acrobat® PDF format from the BC Ministry of Energy, Mines and Petroleum Resources website at http://www.em.gov.bc.ca/Mining/Geolsurv/Publications/catalog/cat_fldwk.htm

Puntzi Lake road, transects the south-central and western parts of the map area. Hundreds of kilometres of secondary logging roads branch off the major forestry trunk roads. Many of these are decommissioned and best accessed by mountain bike or, where extensively degraded or overgrown, on foot. Many roadbeds are partly constructed on glaciolacustrine deposits, which are common at low elevations (*see* 'Surficial Deposits' section). During dry spells this material forms smooth, albeit dusty, roadways. When soaked by rains, however, the clay-rich glaciolacustrine materials turn greasy and travel can be treacherous.

Major drainages include the Clusko and Chilcotin rivers. Both have eroded through Neogene volcanic rocks, exposing older Eocene and Mesozoic rocks. The paleo-Chilcotin River valley probably channelled lava flows in the Chezacut area: this is particularly evident along the river's lower stretches, as can be seen from the Bella Coola Highway (Highway 20) at the spectacular cliffs in Bull Canyon Provincial Park (Gordee et al., 2007). Travellers of this route are left with the impression that the Chilcotin basalts are a thick, widespread blanket, and this impression has negatively impacted mineral exploration within the Interior Plateau.

REGIONAL GEOLOGICAL SETTING AND PREVIOUS WORK

The Chezacut map area is located in the west-central part of the Interior Plateau (Fig 1), in which Mesozoic volcanic-arc strata and their plutonic roots are exposed in a basement high that is draped by Eocene, Miocene and Quaternary volcanic rocks. Results of geological fieldwork presented here build upon the regional geological framework established by Tipper (1969), compiled by Massey et al. (2005) and recompiled with regional revisions by Riddell (2006). To the immediate northeast, in the Clisbako area (NTS 093C/9), Metcalfe et al. (1997) focused on volcanological studies, mapping and determination of potential for epithermal mineralization in the Eocene volcanic rocks. Surficial deposits and glacial physiography have been mapped regionally by Tipper (1971) and in more detail by Kerr and Giles (1993), who also conducted till geochemical surveys (cf. Levson and Giles, 1997). Our 1:50 000 scale mapping is available in hard copy or digital format (Mihalynuk et al., 2008).

FIELD TECHNIQUES

We relied heavily upon 1:20 000 scale digital orthophotographs (0.5 m resolution) for the identification of areas of outcrop and definition of geological lineaments. Remotely sensed, multispectral ASTER imagery that was captured from orbit mid-season was also utilized.

Rocks exposed as a consequence of road construction form only a small percentage of those mapped within the area (only 2.4% of outcrops are within 15 m of roads; Fig 2). Mapping restricted to roadways leaves a negative impression of the percentage of outcrop within the area, probably because rocky areas are avoided in order to minimize road construction costs. Most outcrops are exposed along glacially scoured ridges and along the margins of glacial meltwater channels: both appear as open areas on orthophotographs and ASTER images.

Clast counts in basal till were used locally to help establish geological contacts beneath the till blanket. However, large portions of the western half of the map area are covered by reworked or potentially far-travelled hummocky glacial deposits (Fig 2). In these areas, we have relied upon gravity (Riddell, 2006) and aeromagnetic survey data (Geological Survey of Canada, 1994) to guide our interpretation of unit contacts.

LAYERED ROCKS

Rocks within the Chezacut map area can be assigned to one of four successions: Mesozoic, Eocene, Oligocene–Pleistocene or Pleistocene–Holocene (Fig 3). The presumed oldest rocks are undated, poorly fossiliferous strata that correlate with Late Triassic and Early Jurassic volcanic arc – related strata of the Stikine Terrane (Tipper, 1969; Massey et al., 2005). These arc rocks and their high-level plutonic roots were folded prior to the deposition of widespread Eocene volcanic rocks. Eocene and/or subsequent deformation produced broad folds in the Eocene volcanic strata. Erosion of the deformed terrain during the Miocene created paleotopographic lows into which effusive outpourings of Miocene and younger basalt ponded. The youngest bedrock units probably range from Quaternary to Recent in age, and belong to the alkaline Anahim volcanic belt of possible hot-spot origin (Bevier et al., 1979).

Mesozoic Strata

Volcanic strata of presumed Jurassic age were mapped by Tipper (1969) in three areas: Puntzi Ridge, on the slopes north of Chilcotin Lake and in the Punkutlaenkut Creek area (northwesternmost NTS 093C/08). Rocks north of Chilcotin Lake more closely resemble Eocene strata (an opinion also expressed by Nebocat, 1983); however, we have extended areas of Mesozoic strata in the other two areas on the basis of outcrop found during the 2007 mapping, as well as aeromagnetic and gravity data. We interpret part of Tipper's 'Eocene (?), Oligocene (?)' unit as belonging to the Mesozoic succession, which is exposed in two belts that merge towards Puntzi Ridge, in the southeastern part of the map area (Fig 2).

VARIEGATED LAPILLI ASH TUFF

The most voluminous Mesozoic unit is green or variegated lapilli tuff, which may be more than 1000 m thick. It typically weathers to green or orange angular blocks, with tabular feldspar phenocrysts ≤3 mm in size comprising 15% of the rock. Lapilli are angular to subrounded and tend to be supported by an ash matrix that can contain up to 25% feldspar crystals. Less commonly, clasts are trachytic, with up to 3% subhedral pyroxenes that are <3 mm in diameter, and are quartz-calcite-chlorite amygdaloidal. The unit is of dominantly basaltic andesite composition.

POLYMICTIC BOULDER CONGLOMERATE

Spectacular polymictic boulder conglomerate is exposed on the west flank of Luck Mountain. The most conspicuous clasts are well-rounded boulders of pink monzonite in excess of 1.5 m in diameter. Other major source rock types include feldspar porphyry and lapilli tuff. No calcareous or fine-grained sedimentary rock clasts were identified, suggesting that only the upper parts of the Mesozoic section were exposed to erosion at the time of forma-

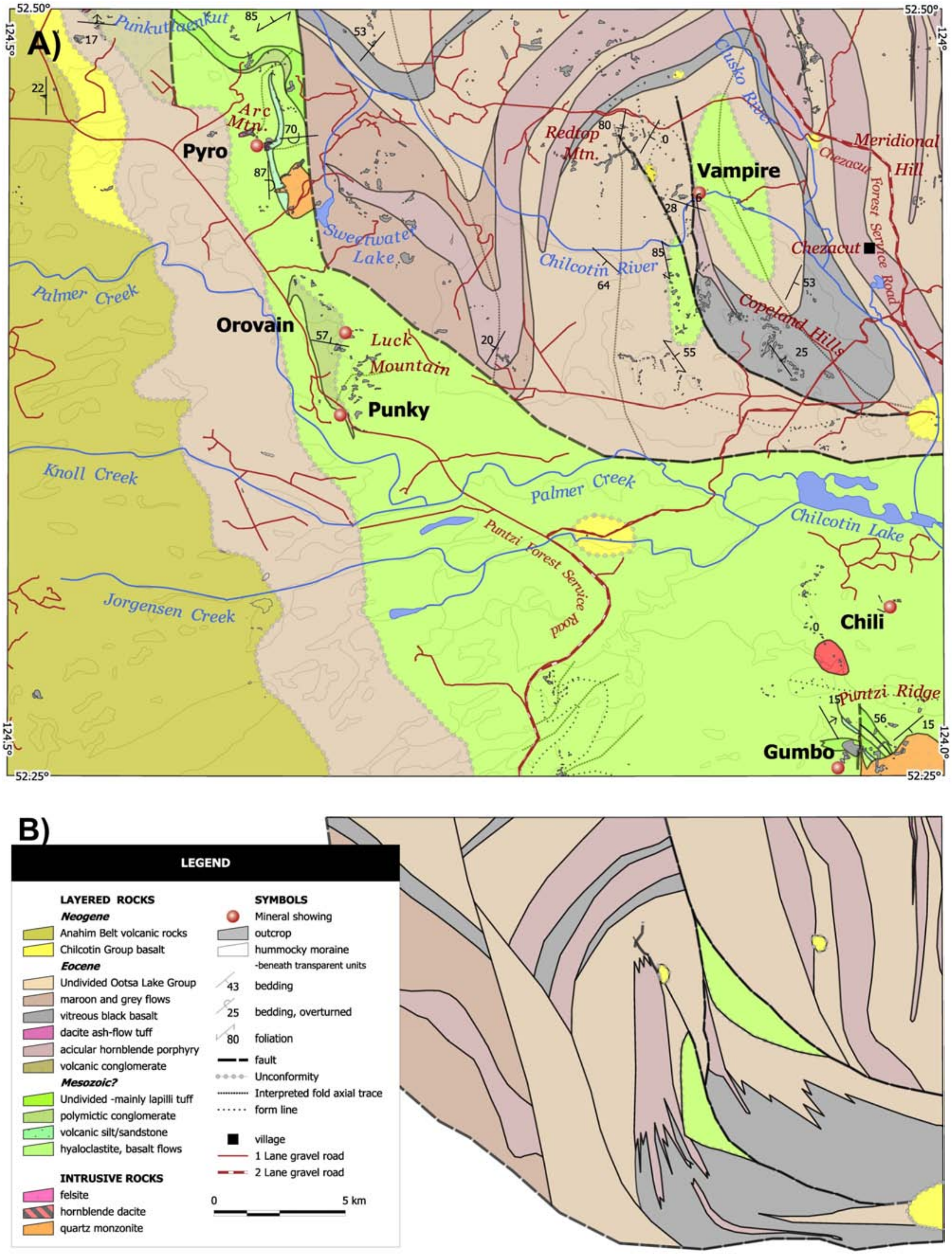

Figure 2. A) Generalized geology of the Chezacut map area. including work by Tipper (1969) and Nebocat (1983). B) Alternative interpretation for the Eocene geology of the map area.

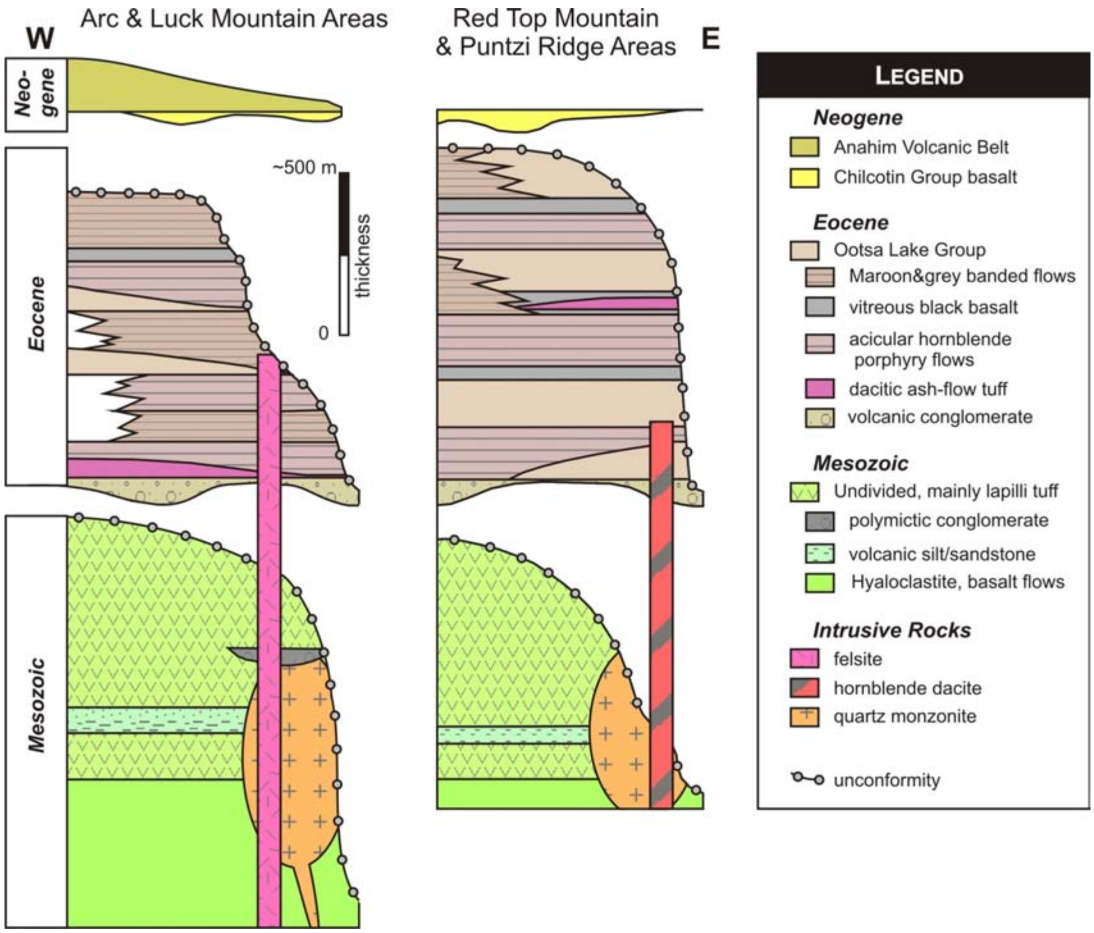

Figure 3. Schematic stratigraphic columns for the northwestern and southeastern parts of the Chezacut map area. Each column shows facies changes from west to east.

tion of this conglomerate. This unit apparently sits above, and grades upwards into, lapilli tuff and tuffite. On this basis, we interpret it as an intraformational conglomerate.

CALCAREOUS FOSSILIFEROUS SANDSTONE

Tan to yellow and rusty-weathering, calcareous volcanic sandstone crops out at one locality on the northern flank of Arc Mountain. Only about 5 m is exposed, and maximum thickness cannot be more than about 50 m. Internal and external moulds of fossil belemnoids (?) and corals are poorly preserved within the coarse-grained feldspathic sandstone. They are best exposed on weathered surfaces, presumably through dissolution of the calcareous fossil. Pyrrhotite, lesser pyrite (up to 4% combined) and traces of chalcopyrite/cubanite and possibly bornite can be observed in hand samples (all sulphides except bornite have been confirmed by petrographic analysis; Fig 4).

Some grains in the sandstone may have a chert protolith, supporting correlation of this unit with the calcareous chert pebble conglomerate unit described below.

CALCAREOUS CHERT PEBBLE CONGLOMERATE

Well-rounded pebbles and granules of white rhyolite typically form white and black conglomerate beds, 1 to 30 cm thick. Together with sandstone interbeds, they form a unit approximately 25 m thick. Other interbeds include siltstone, siliceous volcanic mudstone and hyaloclastite. Conglomerate beds are clast-supported with a recessive, sandy, carbonate-rich matrix. Clasts are up to 4 cm in diameter and well sorted. On the south flank of Arc Mountain, the matrix material of the conglomerate is replaced by mats of tourmaline (Fig 5), perhaps due to a subjacent mass of aplite that forms much of the southwestern flank of Arc Mountain.

HYALOCLASTITE

Bright green hyaloclastite forms a layer approximately 200 m thick near Arc Mountain and in the Puntzi Ridge area. Hyaloclastite typically consists of monomict aphanitic basalt fragments, but may contain fine-grained pyroxene phenocrysts. Clasts are most commonly lapilli sized, ranging up to small blocks. The matrix is sparry calcite, which may locally contain up to 1% pyrite cubes. Near Arc Mountain and in the western Copeland Hills, hyaloclastite passes laterally into massive basalt, possibly pillowed.

BASALT

Dark green, massive, blocky weathering pyroxene basalt is approximately 100 m thick and grades into the hyaloclastite unit. Carbonate-chlorite amygdules up to

1 cm form ≤10% of the rock. Concentric zones with more abundant amygdules are interpreted to parallel pillow margins. Tabular to xenomorphic plagioclase and euhedral pyroxene form ~15% and ~5% of the rock, respectively. Epidote and chlorite-coated joint surfaces are ubiquitous.

VOLCANIC SILTSTONE/SANDSTONE

Green to brown or rust-coloured, commonly recessive, volcanic siltstone and mudstone form a unit approximately 80 m thick. The unit weathers into small (1–5 cm) angular fragments. Rusty zones may contain up to 3% pyrite and/or pyrrhotite. The sedimentary rocks are typically laminated to thinly bedded (1–2 cm). Ripple cross-stratification, scours and flutes, and graded bedding are locally preserved.

Ootsa Lake Group

Volcanic strata of the Eocene Ootsa Lake Group were defined in the Whitesail Lake area (NTS 093E) by Duffell (1959), approximately 200 km northwest of the Quesnel and Anahim Lake areas (NTS 093B, C; Fig 1) where they were mapped between 1954 and 1957 by Tipper (1959, 1969). Metcalfe et al. (1997) conducted revision mapping in NTS area 093C/09 and 16, and 093B/12and 13, which are widely underlain by correlative strata. The southwestern corner of this four-sheet block is the Clisbako sheet (NTS 093C/09), located immediately north of the Chezacut sheet (NTS 093C/08). Metcalfe et al. (1997) renamed the Ootsa Lake Group in this area to 'Clisbako volcanics' and published isotopic age determinations ranging from ca. 53.4 ±0.6 Ma to ca. 44.2 ±0.4 Ma, in agreement with palynological age data. Map units identified as part of the Chezacut project do not easily fit with the assemblages defined across the map boundary by Metcalfe et al. (1997), probably because of the paucity of data observation points that Metcalfe et al. (1997) had upon which to base their interpretations. We have therefore retained the broader 'Group' designation of Tipper (1969). We have found it advantageous to map units based upon phenocryst content and texture, rather than on broader unit assemblages. For example, we separate a regionally significant hornblende-phyric unit, which is included by Metcalfe et al. (1997) within their 'pyroxene-bearing assemblage'. This has allowed us to map out units that could be outlining broad folds in the Eocene volcanic rocks.

A minimum composite thickness for the Ootsa Lake Group in the Chezacut map area is shown in Figure 3 as approximately 1.5 km. However, at a location just 20 km north of the map area, the petroleum exploration well CanHunter b22/093-C-09 penetrated Eocene strata from surface to nearly 3800 m (Riddell et al., 2007). Four detrital zircon age determinations on well cuttings confirm Eocene

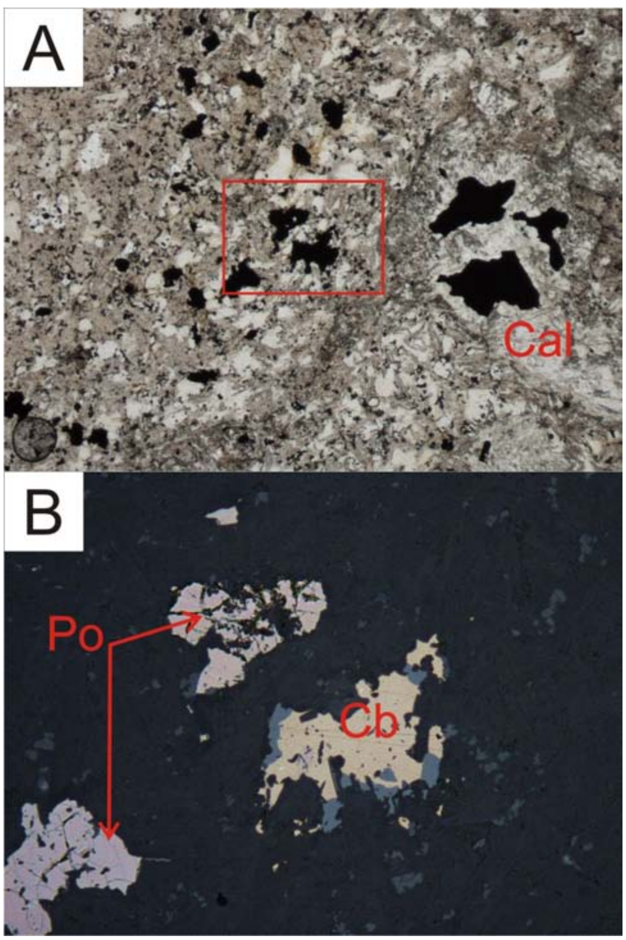

Figure 4. Photomicrographs of thermally metamorphosed calcareous volcanic sandstone on the northeast flank of Arc Mountain: A) calcite (Cal) and intergrown secondary tremolite are conspicuous in transmitted cross-polarized light; B) reflected light shows skeletal pyrrhotite (Po) and cubanite (Cb). Width of rectangle in A represents approximately 1 mm and shows the extent of photograph B.

Figure 5. Tourmaline and silica replacing the matrix within rhyolite pebble conglomerate.

TABLE 1. CHARACTERISTICS FOR DISTINGUISHING BETWEEN VOLCANIC-DOMINATED SUCCESSIONS WITHIN THE CHEZACUT MAP AREA.

	Chilcotin Group	Ootsa Lake Group	Mesozoic Strata
Composition	Mainly basalts	Glassy basalt to dacite	Mainly andesitic
Vesiculation	Highly vesicular – spongy	Amygdaloidal, some vesicles	No vesicles – amygdules only
Magnetic Susceptibility	4.5 ±1.7 (1σ)	3.5 ±4 (1σ); sediment/tuff ~1; flows 1–17	3.9 ±6.4 (1σ); tuffite/tuff 0.1–18; flows 1–20
Alteration	Unaltered – olivine and feldspars vitreous	Feldspars turbid, olivine altered, pyroxene-hornblende are fresh	Feldspars sericitized, ±chlorite-epidote altered; no unaltered olivine; pyroxene epidote-chlorite altered
Deformation	Warping, local high-angle faults	Broad folds, local spaced cleavage, weak foliation	Tight folds, overturned, foliation common

ages down to 3745 m; all dates are equivalent within the limits of error (ca. 52 ±2 Ma; Riddell et al., 2007).

DISTINGUISHING FEATURES

The Ootsa Lake Group volcanic rocks can be difficult to distinguish from Mesozoic volcanic rocks; however, they are typically less altered, lacking the pervasive epidote-chlorite alteration typical of the Mesozoic strata. Some mafic units, especially an olivine-phyric unit near the base of the Ootsa Lake Group, can be mistaken for Chilcotin Group basalt; however, the latter is generally unaltered, with vitreous feldspars, and tends to be highly vesicular. Ootsa Lake Group volcanic rocks, on the other hand, have cloudy feldspars, are clay-chlorite altered, and are amygdaloidal (Table 1).

Basal portions of the Ootsa Lake Group lie with angular unconformity atop Mesozoic rocks. Details of the stratigraphy vary from place to place, but the following generalized succession can be described for the five most important units:

- poorly exposed basal conglomerate
- recessive, maroon-brown flows and breccias, herein termed the Peaty unit
- acicular hornblende porphyry flows (through to all but the very highest levels)
- ‘maroon and grey flow-banded’ and ‘vitreous black’ units (both interlayered with the acicular hornblende porphyry unit)

BASAL CONGLOMERATE

Biotite-rich basal conglomerate is a recessive unit at the base of the Ootsa Lake Group. It is typically yellow to white weathering, poorly indurated, feldspathic and clast supported (Fig 6). It locally grades into coarse-grained sandstone. Euhedral biotite booklets up to 0.5 cm in diameter are characteristic of this unit, commonly forming up to 10% of the rock, either as single crystals within the sandy matrix or as phenocrysts in dacitic clasts. Sandy beds may display reverse grading (interpreted as a water-laid tuffaceous component), scouring and crossbedding. Green clasts, probably derived from the underlying Mesozoic units, are conspicuous and may form up to 30% of the rock.

PEATY BASALT

The Peaty basalt unit is composed of flows and related breccias. Weathered surfaces are a peat-brown colour. Fresh surfaces are dark grey and may display coarse, black, subidiomorphic olivine and idiomorphic, ochre-weathering sanidine (?), each forming up to 2% of the rock. Very fine-grained carbonate is pervasive within the matrix but is not visible as discrete veins or patches, except as amygdules that are otherwise composed of green and amber, chalcedonic quartz. Amygdules are present in vesicu-

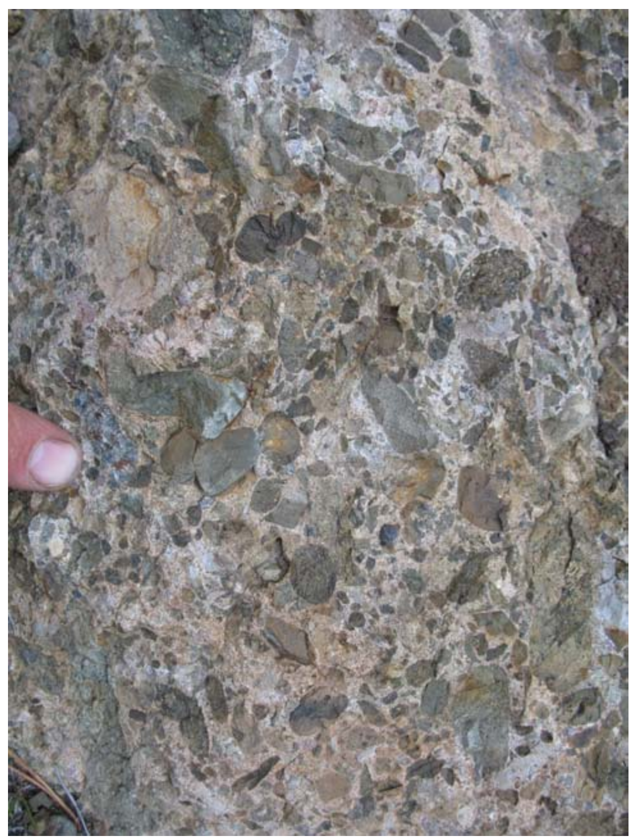

Figure 6. Basal conglomerate of the Ootsa Lake Group. Some of the dark green clasts may be derived from the underlying Mesozoic volcanic strata. Biotite crystals are abundant within the matrix and in Eocene (?) clasts.

lar flow tops, which are developed in the top 1.5 m of the approximately 10 to 70 m thick sequence of flows and breccia that forms this unit.

ACICULAR HORNBLENDE DACITE

Northeast of Arc Mountain, acicular hornblende dacite flows are probably deposited directly atop the Triassic–Jurassic succession. Acicular hornblende porphyry is the dominant exposed rock type in the eastern parts of the map area. It is resistant, commonly underlying ridges. Hornblende displays trachytic alignment within well-developed layers, which are interpreted as flow banding. Parting along flow band surfaces causes the outcrops to break into thin plates that are typical of this unit. Slopes adjacent to outcrops are covered by tan to pink or rusty, angular, poker-chip scree. Fresh surfaces are pinkish tan to grey and display black hornblende needles that are generally less than 4 mm long and form less than 3% of the rock. Typically, hornblende is less than 1%, altered to a punky brown and best displayed on weathered parting surfaces. Salmon-coloured idiomorphic crystals of sanidine (?) locally form up to 2% of the unit.

Two variants of this unit occur locally. One contains coarse hornblende comprising about 5% of the rock. It may display variegated flow bands and flattened pumice lapilli. The other is strongly rusty weathering and limonite and jarosite (?) stained, and is best exposed on the eastern slopes of Redtop Mountain.

Where well exposed, dense flow and vesicular flow-top facies can be identified (Fig 7). Flows range from a couple of metres to perhaps ten metres in thickness, with the top 0.5 to 2 m highly vesicular and recessive weathering. Interflow and autobreccia are well developed in some localities.

AMYGDALOIDAL PYROXENE-PHYRIC BASALT

Brown-green, rubbly weathering, highly vesicular, sparse pyroxene (~2 mm, <3%) and fine plagioclase porphyry is commonly brecciated and forms irregular layers and lenses. Green and amber amygdules of chalcedonic quartz are characteristic. Amygdules are commonly elongate and can be more than 10 cm long. Irregular cavities more than 30 cm in diameter are lined with terminated quartz crystals or filled with geopetal layers of varicoloured (mainly white or amber) chalcedony. This unit is interpreted as a succession of gas-rich basalt flows infilling an irregular topography.

OCHRE BRECCIA AND FLOW LOBES

Ochre-weathering breccia can form layers more than 10 m thick. Dominant clast types are black or maroon, scoriaceous to nonvesicular, aphanitic to rare crowded tabular feldspar porphyries. Pyroxene crystals are a common but minor constituent. Ochre staining and clay alteration may be developed within en échelon tabular zones inter-

Figure 7. Platy-weathering dacitic acicular hornblende-phyric flow unit with characteristic pinkish colour. Photo shows an example of a vesicular flow top, which are not commonly exposed.

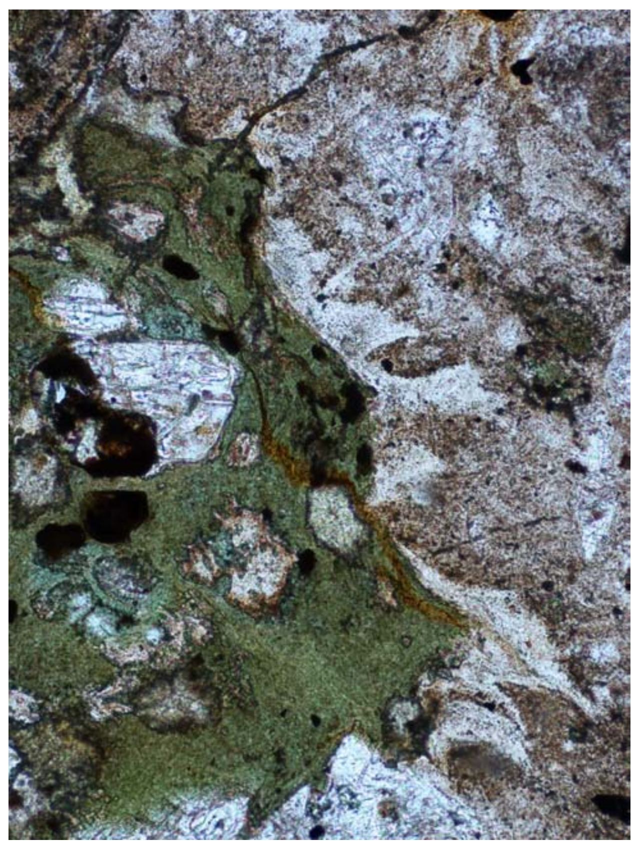

Figure 8. Flattened pumice blocks and possible weak welding producing flame-like textures (F) in chlorite-altered (Chl) hornblende-biotite dacite (quartz, hornblende and biotite phenocrysts fall outside the field of view). Diameter of circle around the crosshairs is ~200 μm.

preted as fumarole fissures. These may be filled with secondary breccias. At one locality in the northeastern part of the map area, agglutinated, flattened blocks of black obsidian are interpreted as part of a spatter breccia. Dense, brown to black lobes are interpreted as fingers of basalt flows within the breccia-dominated unit.

DACITE ASH-FLOW TUFF

White, blocky-weathering hornblende-biotite dacite forms a layer up to approximately 100 m thick. Idiomorphic hornblende and biotite form up to 15% of the unit in subequal amounts. Flattened blocks interpreted as collapsed pumice may display local weak welding (Fig 8) and are suggestive of an ash flow origin. This unit crops out at four localities between the northeastern corner of the map area and west of Redtop Mountain (two are large enough to be shown on Fig 2). These isolated ash-flow tuff layers are interpreted as penecontemporaneous, or deposited during one ignimbritic eruptive episode. Two other occurrences of this unit are located within different stratigraphic intervals and are unlikely to have been deposited during the same eruptive episode.

MAROON AND GREY BANDED RHYOLITE

A ridge-forming rhyolitic unit composed of alternating, millimetre-thick, maroon and grey flow bands (Fig 9) is an attractive and easily distinguished rock type within the north-central part of the map area. It is interlayered with flow top/bottom breccias of the same composition. Most commonly it is aphanitic, but feldspar phenocrysts locally form up to 1% of the rock. The unit is interpreted as a series of low-relief dacitic flow domes.

Figure 9. Typical outcrop of maroon and grey flow-banded unit.

VITREOUS BLACK DACITE

Vitreous, black, sparse pyroxene porphyritic dacite flows and breccia display a distinctive yellow-tan pelagonite rind where weathered surfaces are well developed (Fig 10),

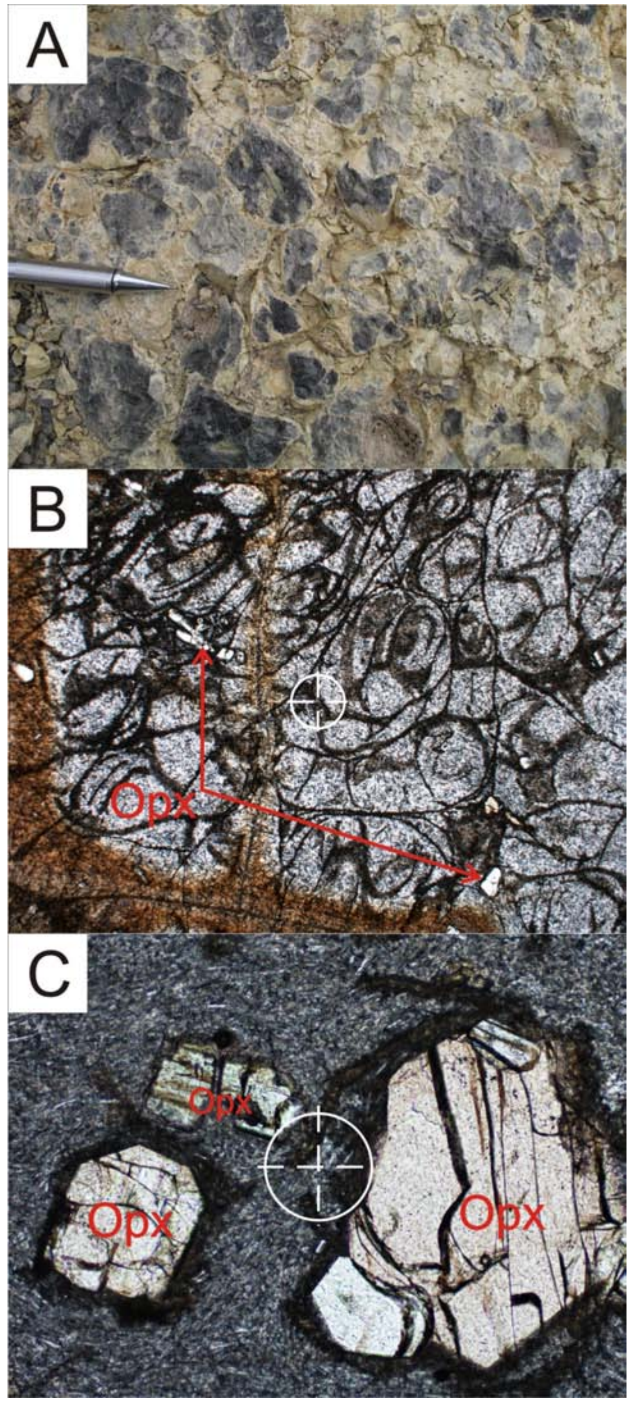

Figure 10. A) Typical pelagonite alteration within vitreous black basalt. (B) Perlitic fracturing and pelagonite alteration along joint surfaces. (C) Plagioclase microlites in glassy matrix surrounding orthopyroxene (? orthoferrosilite) phenocrysts. Circle at crosshairs in photomicrographs is ~200 μm in diameter.

such as among the roots of ubiquitous dead and blown-down pine trees. Phenocrysts include <1% fine, bright green orthopyroxene as anhedral and granular aggregates less than 2 mm in size, and <1% transparent, lath-shaped plagioclase up to 4 mm in size (Fig 9). Euhedral black pyroxenes (up to 1 cm and 1%) were identified within a single flow of this unit. Flow tops are commonly vesicular (less than 5 mm thick, 30% irregularly shaped vesicles), with vesicles lined by yellow-orange to tan mineral aggregates. Interflow breccia facies are less commonly developed.

Neogene Volcanic Rocks

Neogene volcanic rocks encompass two broad rock packages: the Late Oligocene to early Pleistocene Chilcotin Group, which extends over 50 000 km^2 of the Interior Plateau of British Columbia between the Coast Mountains and the Quesnel Highlands (Bevier, 1983b), and the Pleistocene to Holocene Anahim volcanic belt (Mathews, 1989). The Chilcotin Group is composed of submarine and subaerial basalts and associated pyroclastic and sedimentary rocks deposited in a back-arc basin (Bevier, 1983a; Anderson et al., 2001), whereas the Anahim belt rocks are attributed by Bevier (1989) to a hot spot that tracked eastward, with the easternmost volcanic manifestations in the Wells Grey area (Fig 1). However, a swarm of earthquakes in a formerly aseismic region near Nazko cone (Fig 1) may be caused by the movement of magma at depths of approximately 20 km (Pynn, 2007), calling into question simple passage of the hotspot.

CHILCOTIN GROUP

The Chilcotin Group was first described in south-central British Columbia by Tipper (1971) and later redefined by Bevier (1983b) and Mathews (1989). The lava plateau formed from a series of topographically low shield volcanoes that amalgamated into a single, flat terrain. Vents for Chilcotin basalt flows appear to be represented by six basaltic and gabbroic plugs intruded into the flows (Bevier, 1983a), none of which occur within the map area. The Chilcotin Group postdates most tectonism within the area, although regional tilting is reported along the southwest flank of the Interior Plateau (Parrish, 1983).

Chilcotin Group basalt flows rest unconformably on all older rock units. They consist mainly of thin (2–15 m thick), flat-lying, dark brown to grey, columnar-jointed pahoehoe flows. Outcrops in the Chezacut map area are mainly massive or columnar-jointed flows, locally displaying flow-parallel layers of vesicles, or vesicle pipes (Fig 11). These vesicle pipes are a common feature reported by Bevier (1983a), suggesting that the extruded lavas were rich in volatiles.

The average composite thickness of the Chilcotin Group, according to Bevier (1983a), is 67 m, with a maximum known thickness of 141 m. However, 500 m of 'mafic volcanics' were penetrated by petroleum exploration well CanHunter b-16-J/93-B-11 in the Nazko River area, about 60 km east-northeast of the Chezacut map area (Riddell et al., 2007). A preliminary thickness model for the Chilcotin Group indicated that it is less than 25 m thick across approximately 80% of its extent, and more than a third may be less than 5 m in thickness (Mihalynuk, 2006; readers interested in more refined thickness models are referred to Andrews and Russell (2007) and subsequent publications by those and affiliated authors). Despite its limitations, the preliminary thickness model is consistent with the basalt observed in the Chezacut map area, where only six areas with Chilcotin outcrop were found (Fig 2), even though the Chezacut map area is located near the centre of the approximately 50 000 km^2 extent of the Chilcotin Group (Massey et al., 2005).

Anahim Volcanic Belt

Northwest of the Chezacut map area, relict stratovolcanos of the Rainbow, Itcha and Ilgatchuz ranges are products of the compositionally diverse Anahim volcanic belt. Volcanic units include alkaline basalts like hawaiite and basanite, and peralkaline rhyolite and phonolite (Souther and Souther, 1994) of mainly Pliocene and Pleistocene age (Bevier, 1989). Previous petrogenetic studies have focused primarily on the hawaiites (Stout and Nicholls, 1983; Charland et al., 1995), which appear to be derived from the mantle at the base of the crust.

Rocks of the Anahim volcanic belt are sporadically exposed along the western margin of the Chezacut map area. A hill in the southwestern part of the area is underlain by shallowly east-dipping black or pinkish grey, fine to medium-grained, crystal-rich trachybasalt flows. Petrographic analyses of the latter show them to contain conspicuous skeletal olivine with inclusions of devitrified melt (Fig 12A).

Broken outcrops on an isolated knob along the western border of the map area at the headwater of Palmer Creek are composed of light green and grey-weathering basalt. The

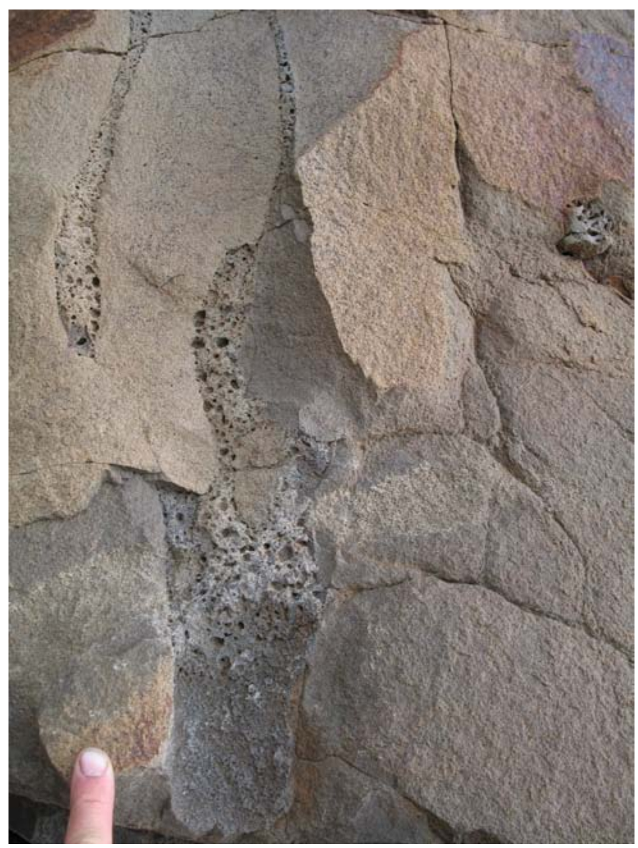

Figure 11. Vesicle pipes, like those shown here, form within and between metre-thick columns of the Chilcotin Group basalt flows.

light green colour is imparted by an approximately 10% aegirine content and a predominance of alkali feldspars (Fig 12B).

A knob 7 km west-northwest of Arc Mountain is underlain by well-developed alternating layers of scoria and flows (Fig 13). Exposures at the lowest elevations are pink tuff with sparse euhedral quartz eyes. Above a covered contact is an approximately 10 m thickness of crowded, coarsely bladed feldspar porphyry flows. On the incised western flank of the knob are beautifully exposed scoria layers (Fig 13) containing lapilli to breccia-sized feldspar crystals (Fig 13, inset) and interlayered, dark grey, sparsely feldspar-phyric flows. These strata dip west, indicating that an elevated magma source was located to the east prior to glaciation.

All exposures of Anahim volcanic belt rocks are mantled by a thin veneer of fluvially modified glacial deposits. Therefore, they predate the latest glaciation. Glacial erratics of Anahim volcanic belt rocks are commonly more than a metre in diameter. One of the most conspicuous rock types that forms these erratics is coarse-grained K-feldspar porphyry with quartz 'eyes' up to 3 cm in size.

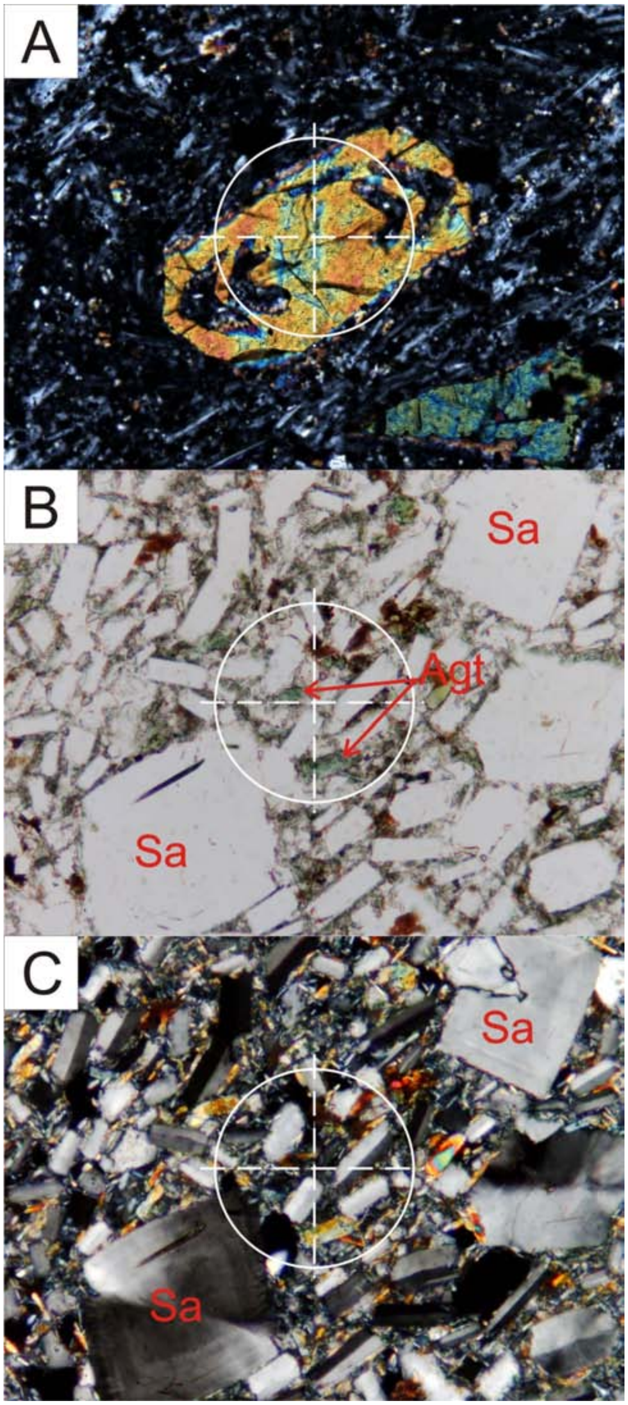

Figure 12. Photomicrographs of A) skeletal olivine that has trapped melt (now devitrified) during rapid growth (cross-polarized light); and B) and C) aegirine (Agt) and Baveno-twinned sanidine (Sa) within a phonolite flow (?) of the alkalic Anahim volcanic belt in plane polarized light (B) and cross-polarized light (C). Circle at crosshairs in photomicrographs is 200 μm in diameter.

SURFICIAL DEPOSITS

Till, glaciofluvial and glaciolacustrine deposits are widespread within the Chezacut map area. These deposits have been discussed as part of a study by Levson and Giles (1997), and were mapped by Kerr and Giles (1993). Readers interested in surficial geology should refer to these publications, as we discuss relatively few salient points here.

Undisturbed basal till is not abundant within the Chezacut map area. The most widespread unit is hummocky moraine, interpreted to have been deposited mainly during ice retreat. Where present, however, basal till is a reasonable proxy for the local bedrock geology through geochemical analysis of the silt fraction and composition of the entrained clasts. Geochemical analyses are reported in Peat et al. (2008). One notable sample is MMI07-20-4 (52.4609°N, 124.0849°W), which contains significant Ag (6 ppm).

Glaciolacustrine deposits are widespread within the Chezacut map area. They extend up to a consistent elevation of approximately 1150 m across the area (Fig 14), and are interpreted to have been deposited from a late glacial lake that inundated approximately 65% of the map area at its peak level.

Figure 13. Eroded flank of an Anahim volcanic belt stratovolcano. Inset photo demonstrates the very coarse size attained by the feldspars within these units.

INTRUSIVE ROCKS

Three intrusive bodies, each approximately 1 km in diameter, crop out in a northwest-trending belt in the map area. From south to north, these are the Puntzi Ridge quartz monzonite, the Chili dacite, and the 'Sweetwater Lake' monzonite. The latter informal name is taken from a kilometre-long, deep lake 3 km southeast of Arc Mountain (Fig 2).

Puntzi Ridge Quartz Monzonite

Pink to grey quartz monzonite crops out on the southeastern flank of Puntzi Ridge and 'Sweetwater Lake'. Composition varies from quartz diorite to monzodiorite and grain size varies from medium to coarse. Mafic minerals include biotite and subordinate hornblende. Late fractures in the monzonite at Puntzi Ridge are commonly annealed with K-feldspar and display pink halos that are 2 cm or more wide (Fig 15A). Chlorite±epidote alteration and coatings on late joint surfaces affect most parts of the intrusions to some degree.

Dikes of monzodiorite extend from the main body at 'Sweetwater Lake', and a varitextured diorite apophysis is locally foliated. Thermal metamorphic halos affect Mesozoic country rocks for at least 30 m from the intrusive contacts, but some of the Mesozoic units may postdate intrusion of the bodies. For example, a biotite-bearing dacite/latite tuff at Puntzi Ridge is, in places, almost indistinguishable from the intrusion (Fig 15B) and, on this basis, is interpreted as a coeval extrusive equivalent. However, latest phases of the intrusion may cut volcanic units at

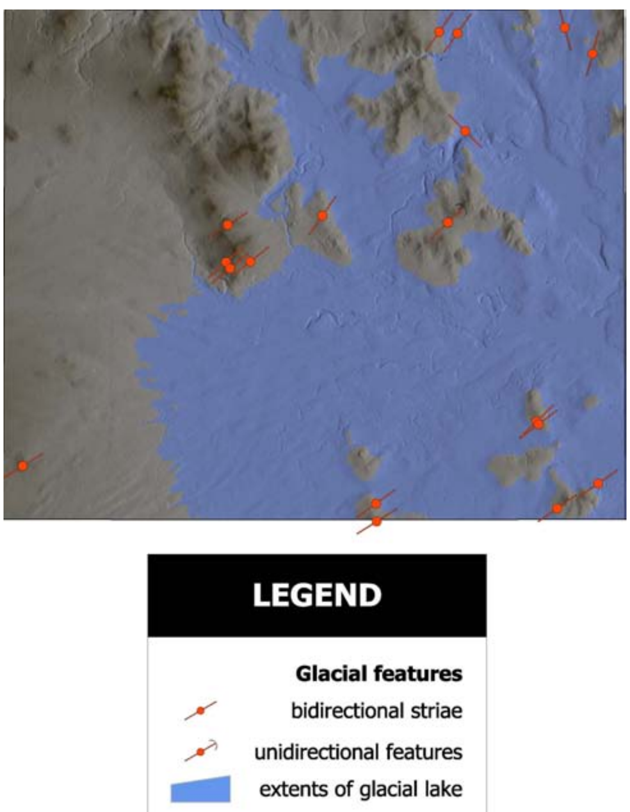

Figure 14. Distribution of glaciolacustrine deposits within the Chezacut map area is consistent with an enormous glacial lake having a surface elevation of 1153 m, which would have inundated approximately 65% of the map area.

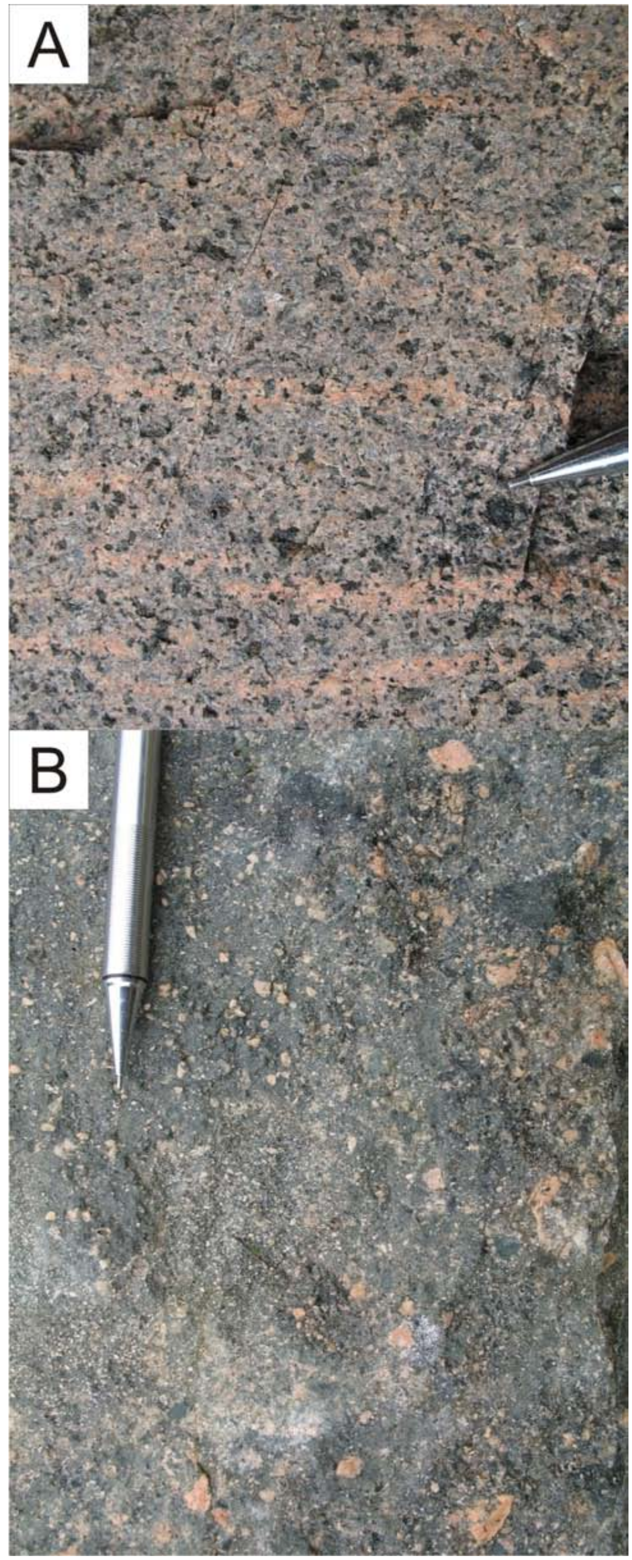

Figure 15. A) K-feldspar alteration halos on parallel fractures within Puntzi Ridge quartz monzonite. B) Quartz monzonite tuff interpreted as comagmatic with the Puntzi Ridge quartz monzonite.

stratigraphic levels higher than the dacite/latite tuff. Samples of the plutons were collected for isotopic age determination. The extensively altered ‘Sweetwater Lake’ pluton was sampled for U-Pb zircon/titanite determination(s), and one of the rare zones of fresh biotite and K-feldspar in the Puntzi pluton was sampled for $^{40}Ar/^{39}Ar$ age determination.

Chili Dacite

Porphyritic dacite crops out sporadically across an approximately 200 m by 1000 m area, about 3 km northwest of Puntzi Ridge. It is white to grey-weathering and medium-grained, composed of ~2% euhedral hornblende and ~15% biotite booklets, as well as equant white feldspar, possibly sanidine. In one of the highest exposures, an ~100 m long zone contains quartz-lined miarolitic cavities up to 2 cm across, knots of coarse biotite and abundant xenoliths (probably autoliths).

The Chili dacite is lithologically similar to dikes and ash-flow tuff units within the Ootsa Lake Group, and is therefore considered as a potential subvolcanic feeder. To test this correlation, a sample containing fresh biotite was collected for $^{40}Ar/^{39}Ar$ age determination.

STRUCTURE AND DEFORMATION

Evidence of deformation can be found in rocks of all ages within the Chezacut map area. Deformation is most intense in the oldest rocks — folded strata of presumed Mesozoic age. However, even rocks that may be as young as Quaternary display evidence of contractional deformation. Mesozoic rocks are dominated by massive volcanic strata that do not readily reveal deformational fabrics, but tight folds and overturned beds can be observed where these rocks are interbedded with sedimentary strata. In some areas, a spaced cleavage or weak phyllitic fabric is developed.

Deformation of strata of the Ootsa Lake Group is mainly displayed by variably dipping strata, locally vertical, which are interpreted to outline kilometre-scale folds. An open, north-plunging antiformal culmination is interpreted in the northeastern part of the Chezacut map area. It has a wavelength of at least 15 km and exposes Mesozoic strata in its core. Oppressed limbs have resulted in escape structures, such as sinistral shear zones on the eastern limb and thrust faulting within the fold core. Penetrative, closely spaced cleavage and weak phyllitic fabrics are best developed north of Meridional Hill (Fig 16A) and in the Copeland Hills where they extend across 50 to 200 m.

Our interpretation of large-scale folds is a departure from the more classic view of widespread block-faulting and extension during Eocene magmatism. In fact, nowhere can we conclusively demonstrate a fold closure by walking volcanic stratigraphy through a fold hinge. The outcrop distribution of the Ootsa Lake Group is sufficiently sparse to easily accommodate a more classic interpretation. For example, Figure 2B presents one of many possible alternative interpretations of the Eocene geology, but it does not explain the spaced cleavage and weak phyllitic fabrics that are exposed in most areas with abundant outcrop.

Within the northwestern part of the map area, Neogene Anahim volcanic rocks display evidence of high-angle reverse faulting (Fig 16B). Inexplicably, the discrete fault

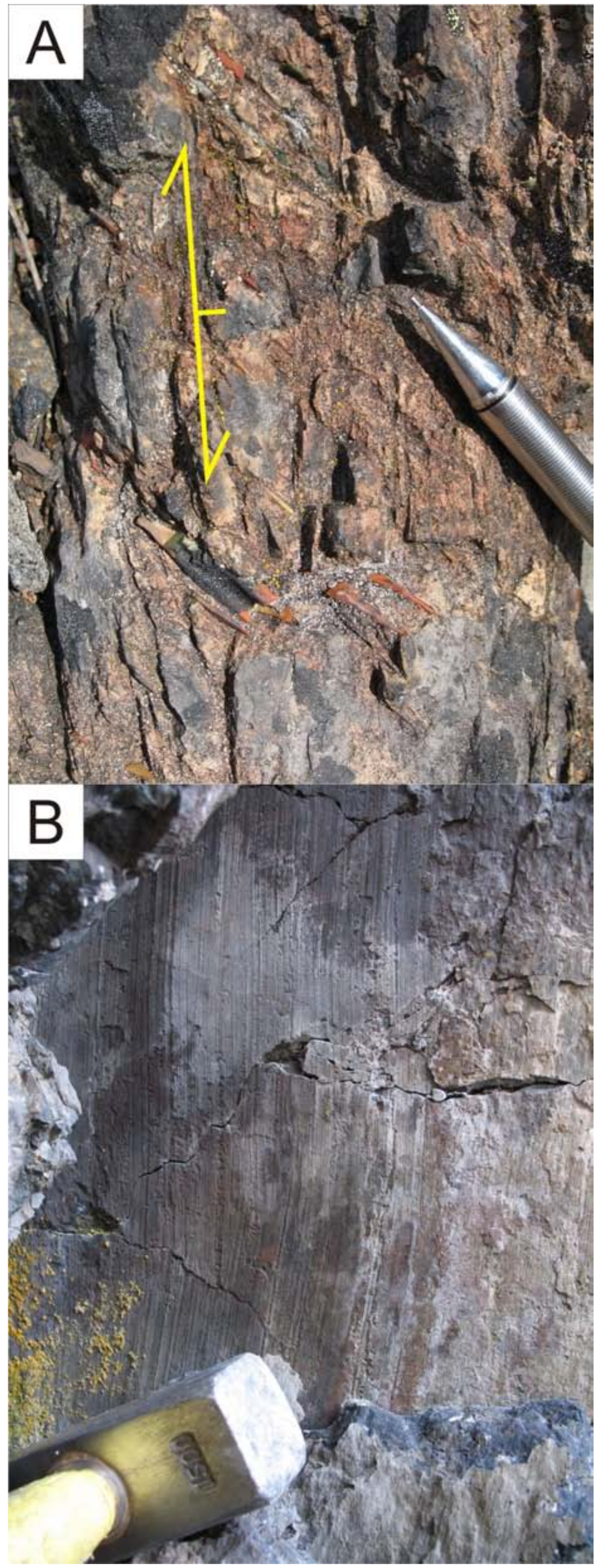

Figure 16. A) Spaced cleavage (oriented parallel to length of photo) pervasively overprints a basalt flow containing elongated amygdules (with pencil aligned). B) Steeply plunging striae on fault surfaces commonly occur within flow units of the Anahim volcanic belt at this locality. Possible causes of the faulting include loading by ice or volcanic deposits, or previously undocumented tectonism.

planes are focused in dense flows, not in the adjacent, less competent scoriaceous layers.

Because of the very low relief and extensive hummocky moraine within the southwestern part of the map area, contacts between the Mesozoic, Eocene and Neogene units are based largely on gravity and aeromagnetic lineaments.

Deformation Age and Significance

The age of pre-Miocene deformation cannot be well constrained within the map area. Possible correlations with deformational events defined outside of the map area are as follows:

- Paleocene–Middle Eocene: Kinematic linkage with 110 km of dextral offset on the crustal-scale Yalakom Fault system (Umhoefer and Schiarizza, 1996), and/or Eocene unroofing of the Tatla Lake metamorphic complex (Friedman and Armstrong, 1988; Friedman, 1992), located 30 km south of the Chezacut map area. Eocene extension is consistent with rapid Early Eocene cooling (55–50 Ma), as determined from apatite fission track studies in the region (Riddell et al., 2007).
- Middle Jurassic (Bajocian): Emplacement of the Cache Creek Terrane (Ricketts et al., 1992; Mihalynuk et al., 2004). Cache Creek rocks are juxtaposed with Mesozoic strata about 80 km to the east.

A sub-Eocene structural discontinuity is interpreted because the younger strata are not observed to be isoclinally folded (although flow fabrics displaying all manner of folding are common within Tertiary units of dacitic and rhyolitic composition, they are not tectonic in origin). In addition, a sandstone and conglomerate unit containing clasts of the Mesozoic unit is interpreted as a sub-Eocene basal conglomerate. It also contains vitreous, euhedral, biotite booklets and 'dacitic' clasts containing biotite, probably attributable to syndepositional volcanism. Samples of this biotite were collected for isotopic age determination. The occurrence of biotite may mark the onset of volcanism of the Ootsa Lake Group in this area, constraining the age of the angular unconformity to early Eocene.

MINERALIZATION

Prior to 2007, only a single MINFILE occurrence was reported for the Chezacut area. Identified as MINFILE 093C 011 (MINFILE, 2007), the Chili (formerly Punt) occurrence is a shear-related quartz stockwork with argentiferous and auriferous chalcopyrite (Nebocat, 1983; see also new analysis 1.5 ppm Au and 69 ppm Ag in Table 2b) within probable Mesozoic volcanic strata (Fig 2). The quartz stockwork cuts epidote-chlorite-altered feldspar-pyroxene porphyry and lapilli tuff. The quartz is greasy grey in places, probably related to its elevated Ag content.

During the course of our work, five new mineral occurrences were discovered. From north to south these are the Pyro, Orovain, Punky, Vampire and Gumbo showings. Coarse-grained pyrolusite-rich breccias dominate isolated outcrops at the Pyro showing. Both the Punky and Orovain occurrences are copper sulphide and native copper – bearing veins. Mineralization at the Vampire and Gumbo showings is disseminated copper sulphides in altered igneous rocks.

Pyro Showing

The Pyro showing is located at the southwestern base of Arc Mountain (Fig 2). This area is part of a thermally metamorphosed zone characterized by silicification and secondary tourmaline in outcrops exposed for more than 350 m along a glacial outflow channel. Tourmaline grains provide a nucleation site for nonpleochroic hexagonal crystals that grow in optical continuity with the tourmaline and replace up to 50% of the rock matrix (Fig 17). Mineralization at the Pyro showing is not well exposed but, over a 10 m by 25 m area, it consists of sooty, rust-coloured, coarse-grained breccia with hematite-goethite-pyrolusite-rich cement (>1% Mn, the analytical upper concentration limit for determination of this element by the ICP-MS method; *see* Table 2a) and vein-like bodies up to 35 cm thick. A low-angle fault zone that cuts the mineralization is tentatively interpreted as a top-to-the-southeast thrust fault.

Analysis (Table 2a, b; results to two significant figures for INAA and ICP-MS values, respectively) of two samples of sooty mineralization, including a chip sample at 20 cm intervals across 4 m (sample MMI07-48-4B), reveal elevated values for Au (90, 160 ppb), As (530, 1200 ppm), Sb (34, 6 ppm) and Zn (840, 3000 ppm); and, for ICP-MS analyses only, 11 ppm Ag, 30 ppm Bi, 2.3 ppm Tl and 13 ppm Te. Most surprising is Te enrichment, which is more than 4000 times the average crustal abundance in analogous volcanic-arc rocks (Yi et al., 2000). Conclusive classification of this deposit is not possible given the cursory nature of our observations; however, in consideration of the tourmaline and silica alteration and induration, a skarn origin is possible. If so, the aplite body that forms much of the southwestern flanks of Arc Mountain is the likely cause of the thermal-metamorphism. Silver-zinc-lead skarns are commonly enriched in Mn and have elevated Bi and Au (Ray, 1995); however, the Te enrichment is unusual for a skarn. On the basis of elevated Au and Ag values alone, this occurrence warrants further investigation.

Punky and Orovain Showings

Both the Orovain and Punky showings are copper-bearing vein occurrences located near the peak and on the southwestern flank of Luck Mountain, respectively (Fig 2). Mineralization at the Orovain occurrence is within a set of 0.5 to 8 cm thick quartz-epidote-prehnite veins. Veins cut feldspar-phyric lapilli tuff and are generally subparallel and west trending, with a spacing of approximately 1 m, and exposed over a 50 by 75 m area. Mineralization occurs as disseminations of native copper mantled by chalcocite (Fig 18). Copper mineralization is most abundant within the vein material, but sporadically occurs within the alteration envelope adjacent to the vein. Alteration mineralogy of the envelopes is similar to that of the veins, and total envelope thickness is about equal to that of the veins. Analysis of the veins reveals between 1026 ppm and >1% Cu (Table 2a, samples MMI07-37-7, 8 and 9).

Veining at the Punky occurrence is more sporadic with a less well developed vein set than at the Orovain occurrence. Quartz-carbonate veins up to 12 cm thick are copper stained. Preliminary petrographic analysis of the veins reveals no primary copper mineralization; however, calcite-

TABLE 2. SELECTED ANALYTICAL RESULTS FROM MINERALIZED SAMPLES WITHIN THE CHEZACUT MAP AREA: A) SELECTED ICP-MS RESULTS, B) SELECTED INAA RESULTS. A DIGITAL REPORT AND DATABASE OF ALL SAMPLES ANALYZED AS PART OF THE CHEZACUT MAPPING PROJECT ARE AVAILABLE IN PEAT ET AL. (2008).

(a)

Sample number	Sample type	Latitude	Longitude	Cu (ppm)	Pb (ppm)	Zn (ppm)	Ag (ppb)	Fe (%)	As (ppm)	Au (ppb)	Sb (ppm)	Bi (ppm)	Tl (ppm)	Hg (ppb)	Te (ppm)	Mn (ppm)
KTE07-13-12 Punky	Hand - assay	52.3697	-124.3204	1925	2.82	23.5	222	1.80	4.8	0.2	0.08	<0.02	<0.02	21	0.04	535
KTE07-13-8 Punky	Hand - assay	52.3678	-124.3224	1100	13.36	9.7	401	0.79	3.7	0.2	0.07	<0.02	<0.02	<5	0.04	393
MMI07-1-4	Hand - assay	53.4212	-125.7519	98	37.93	83.5	448	14.39	6.8	23.9	2.15	3.78	0.08	13	0.06	1653
MMI07-17-11B Vampire	Hand - assay	52.4403	-124.1284	2839	2.22	55.5	556	2.01	6.4	0.5	0.66	0.04	<0.02	<5	0.07	660
MMI07-17-7 Vampire East	Hand - assay	52.4402	-124.1287	95	1.55	48.4	685	2.88	95.3	8	0.63	0.16	<0.02	6	1.11	514
MMI07-17-8 Vampire	Hand - assay	52.4402	-124.1294	1188	1.41	44.9	266	2.16	39.7	9	0.29	0.02	<0.02	<5	0.63	838
MMI07-17-9 Vampire	1.1 m chip sample	52.4400	-124.1301	2145	1.07	95.9	232	2.63	7.4	1.5	0.19	<0.02	<0.02	<5	0.10	798
MMI07-17-9rep Vampire	1.1 m chip sample	52.4400	-124.1301	2347	1.44	95.4	270	2.62	7.9	0.9	0.23	<0.02	0.02	<5	0.11	811
MMI07-18-6 Chilcotin cutbank	Hand - assay	52.4350	-124.1036	224	504.18	408.0	395	1.29	2.3	44.6	0.10	0.19	<0.02	697	0.04	719
MMI07-37-7	Hand - assay	52.3945	-124.3197	2613	7.84	7.3	296	1.48	9.2	0.4	0.05	<0.02	<0.02	20	0.05	384
MMI07-37-8	Hand - assay	52.3945	-124.3200	>10000	6.10	17.0	3182	1.90	26.7	1.1	0.09	<0.02	<0.02	184	0.03	405
MMI07-37-9	Hand - assay	52.3940	-124.3199	1026	4.15	6.8	58	1.46	2.0	0.5	<0.02	<0.02	<0.02	5	<0.02	194
MMI07-38-7	Hand - assay	52.3824	-124.3140	1928	6.27	42.0	284	3.53	6.7	2.4	0.03	0.04	<0.02	15	0.03	544
MMI07-44-1	Hand - assay	52.2527	-124.0568	196	0.61	32.2	77	2.81	<0.1	1.1	0.02	0.04	0.04	<5	<0.02	356
MMI07-48-4 Pyro	Hand - assay	52.4555	-124.3672	44	475.30	2984.0	11276	7.39	1227.0	163.5	6.46	29.78	0.45	670	12.59	>10000
MMI07-48-4B Pyro	Hand - assay	52.4555	-124.3672	9	30.45	569.0	800	11.21	547.2	9.7	2.36	1.53	2.27	308	0.53	>10000
			Detection limit:	*0.01*	*0.01*	*0.1*	*2*	*0.01*	*0.1*	*1*	*0.02*	*0.02*	*0.02*	*5*	*0.02*	*1*

(b)

Sample number	Sample type	Latitude	Longitude	Au (ppb)	Ag (ppm)	As (ppm)	Ni (ppm)	Zn (ppm)	Sb (ppm)
KTE07-6-6 Chili occurrence	Hand - assay	52.3069	-124.0269	1530	69	15.2	20	470	3.5
MMI07-18-6 Chilcotin cutbank	Hand - assay	52.4350	-124.1036	50	< 5	9.1	<20	480	6.6
MMI07-44-1	Hand - assay	52.2527	-124.0568	<2	< 6	<0.5	150	180	<0.1
MMI07-48-4 Pyro	Hand - assay	52.4555	-124.3672	90	< 7	526.0	130	840	33.8
MMI07-48-4B Pyro	4 m chip sample	52.4555	-124.3672	<2	< 8	249.0	<20	200	10.5
			Detection limit:	*2*	*5*	*0.5*	*20*	*50*	*0.1*

Notes: A full list of samples and elements analyzed can be obtained for both INAA and ICP-MS suites from http://www.em.gov.bc.ca/Mining/Geolsurv/Publications/catalog/cat_geof.htm epidote alteration patches within the tuffaceous host rocks do contain native copper mantled by chalcocite and hematite. These observations suggest that sampling that was biased towards copper-stained vein material may have underrepresented the copper content of the outcrop, and future investigators should look carefully at the tuffaceous host rocks for signs of mineralization. Analysis of the vein material yielded Cu values of between 1925 and 1100 ppm (Table 2a).

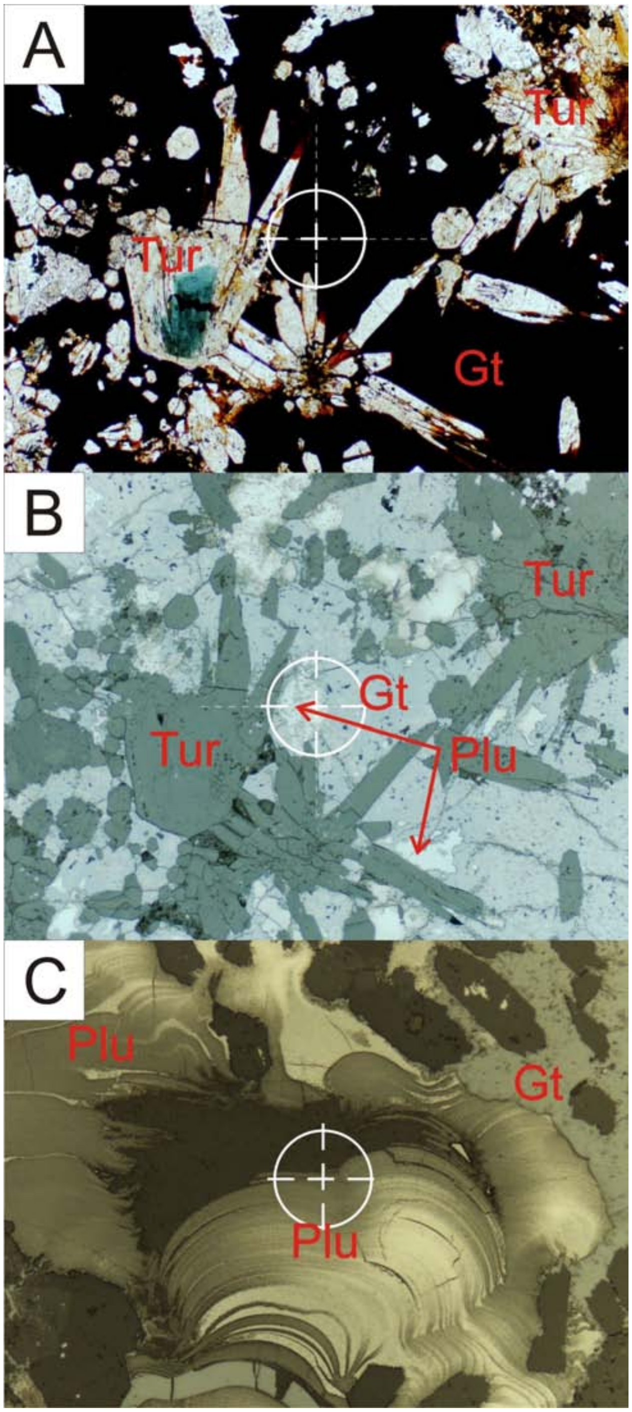

Figure 17. Photomicrographs of mineralization at the Pyro occurrence: A) plane-polarized light shows nucleus of olive-blue pleochroic tourmaline (Tur) overgrown by radiating mat of nonpleochroic tourmaline; B) and C) opaque and semi-opaque minerals are tentatively identified in reflected light (B) as goethite (Gt, red internal reflections), hematite and pyrolusite (Pru) and/or other Fe-Mn oxides) that, in partly uncrossed polarized light (C), display botryoidal and/or geopetal textures. Circle at crosshairs in photomicrographs is 200 μm in diameter.

Gold and silver values at both occurrences are negligible.

Vampire Showing

Disseminated chalcopyrite occurs within a belt of outcrops of mainly intermediate volcanic breccia, located between the old homestead access road and the Chilcotin River, about 5 km above its confluence with the Clusko River (Fig 2). At this locality, epidote-quartz-chlorite-pyrite alteration (propylitization) is widespread in feldsparphyric volcanic breccia and sparse white, dacitic (?) tuff layers (Fig 19), producing green and rust outcrops that extend sporadically for approximately 110 m along the river valley. Analysis of samples with visible chalcopyrite returned values of between 0.12% and 0.28% Cu, including a 1.1 m chip sample across one well-mineralized outcrop that returned 0.21% Cu. No significant Au or Ag enrichment

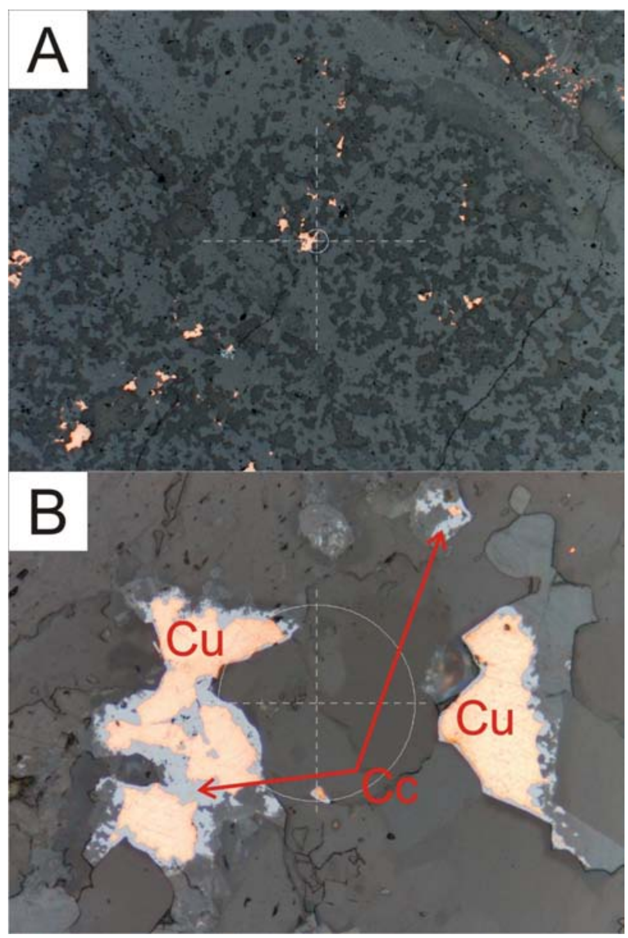

Figure 18. Reflected light photomicrographs of samples of mineralization at the Orovain occurrence showing: A) disseminated native copper within a well-mineralized vein, and B) close-up of a typical native copper (Cu) grain showing a mantle of chalcocite (Cc). Circle at crosshairs in photomicrographs is 200 μm in diameter.

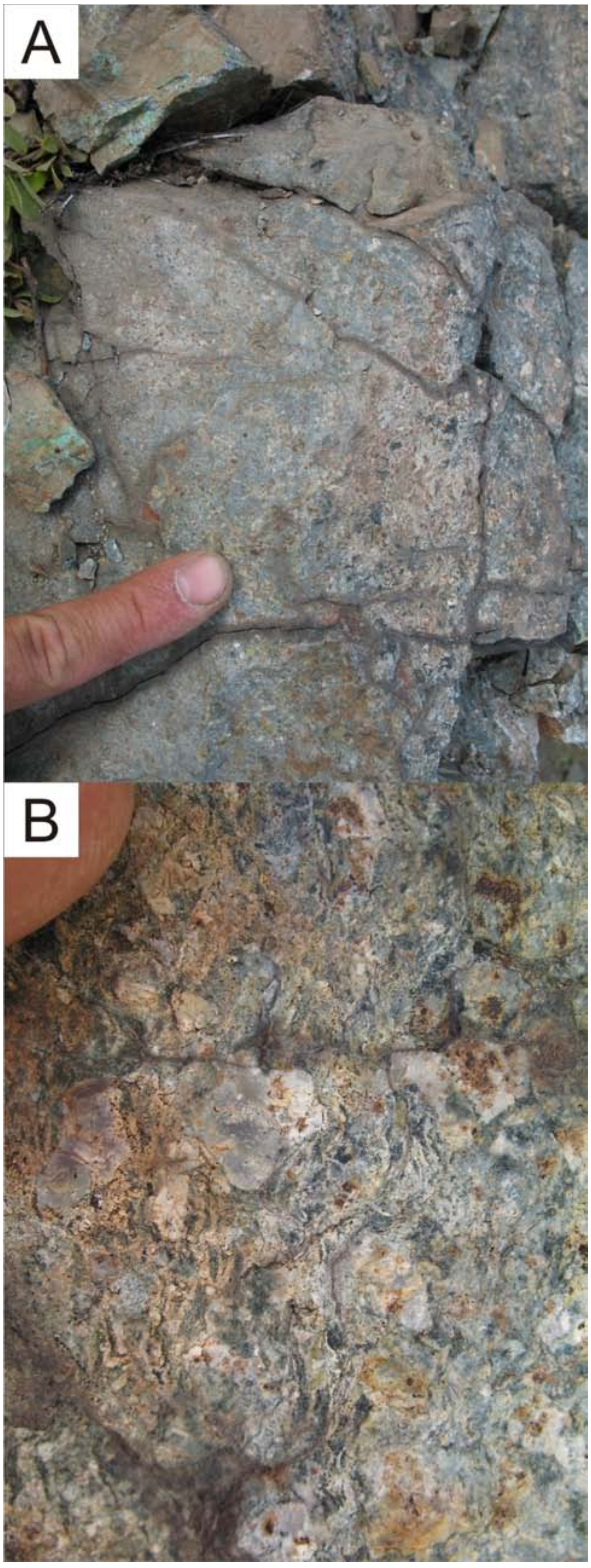

Figure 19. Photographs of the Vampire occurrence, showing: A) an outcrop of intermediate tuff mineralized with chalcopyrite (recessive rusty) and sparsely copper-stained, fresh fracture surfaces; and (B) a thin interbed of felsic tuff.

was detected. Of the chalcopyrite-bearing samples analyzed, the highest Au value returned is 9 ppb and the highest Ag value is 0.5 ppm (Table 2a).

Gumbo Showing

Mineralization at the Gumbo showing occurs as local accumulations of disseminated chalcopyrite and pyrrhotite (Fig 20A) in an altered, porphyritic, mafic igneous unit (Fig 20B). Relict phenocrysts are probably plagioclase and pyroxene. Sporadic low outcrops of this unit are dark green-grey with rust patches (oxidized pyrrhotite), and well indurated with angular, blocky jointing. Samples from the showing returned elevated levels of Cr (518 ppm, possible contamination from mill), Ni (150 ppm) and Zn (180 ppm) relative to other samples analyzed.

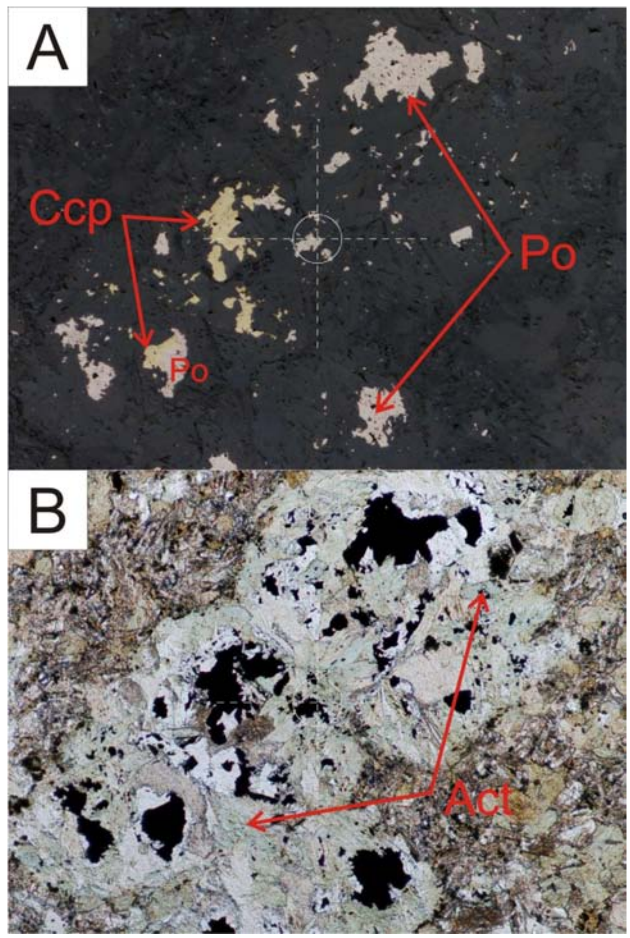

Figure 20. Photomicrographs of altered pyroxene-phyric volcanic or intrusive rock at the Gumbo occurrence, showing A) pinkish pyrrhotite (Po) and yellow chalcopyrite (Cpy) as irregular clots (in places intergrown) and as dustings in the rock matrix (reflected light); and; B) sulphides replacing the cores of altered phenocrysts, possibly pyroxene (plane-polarized transmitted light); pale green actinolite (Act), and chlorite also replace pyroxene (?). Circle at crosshairs in photomicrographs is 200 μm in diameter. Remainder of the rock is hornblende diorite.

SUMMARY

Geological field investigations within the Chezacut map area demonstrated the following:

- Rumours of a relatively unbroken blanket of glacial cover are ill-founded. Bedrock exposure is more extensive than is generally perceived.
- With the aid of detailed digital orthophotos and multispectral imagery, strategies were successfully devised to maximize the chances of encountering outcrops.
- The extent of the Chilcotin Group is much less than anticipated: a 96% decrease in the area originally included in Massey et al. (2005). If the Anahim volcanic belt is included with the Chilcotin Group, there is still a 62% decrease in young volcanic cover.
- Mesozoic strata are more abundant and more extensively intruded than previously thought. If our interpretation is correct, Mesozoic units now account for nearly 240% of the distribution shown in Massey et al. (2005).
- Eocene strata are probably deformed by broad folding, not solely by block faulting. If this interpretation is correct, it appears that Mesozoic strata are exposed in the core of a broad anticline.
- Neogene volcanic rocks are commonly highly vesicular (25%), resulting in lower than expected density (possible gravity lows, not the highs normally anticipated from basalt).
- Significant new mineral occurrences can still be discovered at surface within the Chezacut map area (in our case, within 1.5 weeks of commencing the mapping project).
- Discovery of four new mineral occurrences during the course of the Chezacut regional mapping project is a demonstration of the underexplored status of this area. The region clearly deserves much more exploration attention than it has received in the past.

ACKNOWLEDGMENTS

Larry Diakow helped with geological reconnaissance and introduced our field crew to the nebulous geology of the Nechako Plateau. He also kindly reviewed and improved an earlier draft of this manuscript. Travis Ferbey taught us why, where and how to dig till and mix daiquiris. Our crew was joined near season's end by the highly energetic and helpful Margot McKeown. The parched plateau was made more pleasurable through the kindness of Kevin Newberry of Chezacut Ranch Ltd. We offer our apologies to George Maybee, whose freshly graded dirt road turned to mud and then ruts with the barely controlled passage of our truck.

REFERENCES

Anderson, R.G., Resnick, J., Russell, J.K., Woodsworth, G.J., Villeneuve, M.E. and Grainger, N.C. (2001): The Cheslatta Lake suite: Miocene mafic, alkaline magmatism in central British Columbia; *Canadian Journal of Earth Sciences*, Volume 38, pages 697–717.

Andrews, G.D.M. and Russell, J.K. (2007): Mineral exploration potential beneath the Chilcotin Group (NTS 092O, P; 093A, B, C, F, G, I, J, K), south-central British Columbia: preliminary insights from volcanic facies analysis; *in* Geological Fieldwork 2006, *BC Ministry of Energy, Mines and Petroleum Resources*, Paper 2007-1, and *Geoscience BC*, Report 2007-1, pages 229–238.

BC Ministry of Forests and Range (2005a): The state of British Columbia's forests 2004; *BC Ministry of Forests and Range*, URL <http://www.for.gov.bc.ca/hfp/sof/2004/> [November 2007].

BC Ministry of Forests and Range (2005b): British Columbia's Mountain Pine Beetle Action Plan 2005–2010; Government of British Columbia, 20 pages, <www.for.gov.bc.ca/hfp/mountain_pine_beetle/actionplan/2005/actionplan.pdf> [October 2, 2006].

Bevier, M.L., Armstrong, R.L. and Souther, J.G. (1979): Miocene peralkaline volcanism in west-central British Columbia — its temporal and plate-tectonic setting; *Geology*, Volume 7, Number 8, pages 389–392.

Bevier, M.L. (1983a): Implications of chemical and isotopic composition for petrogenesis of Chilcotin Group basalts, British Columbia; *Journal of Petrology*, Volume 24, pages 207–226.

Bevier, M.L. (1983b): Regional stratigraphy and age of Chilcotin Group basalts, south-central British Columbia; *Canadian Journal of Earth Sciences*, Volume 20, pages 515–524.

Bevier, M.L. (1989): A lead and strontium isotopic study of the Anahim volcanic belt, British Columbia: additional evidence for widespread suboceanic mantle beneath western North America; *Geological Society of America Bulletin*, Volume 101, pages 973–981.

Charland, A., Francis, D. and Ludden, J. (1995): The relationship between the hawaiites and basalts of the Itcha Volcanic Complex, central British Columbia; *Contributions to Mineralogy and Petrology*, Volume 121, pages 289–302.

Duffell, S. (1959): Whitesail Lake map area, British Columbia; *Geological Survey of Canada*, Memoir 299, 119 pages.

Friedman, R.M. and Armstrong, R.L. (1988): Tatla Lake metamorphic complex: an Eocene metamorphic core complex on the southwestern edge of the Intermontane Belt of British Columbia; *Tectonics*, Volume 7, pages 1141–1166.

Friedman, R.M. (1992): P-T-t path for the lower plate of the Eocene Tatla Lake metamorphic core complex, southwestern Intermontane Belt, British Columbia; *Canadian Journal of Earth Sciences*, Volume 29, pages 972–983.

Geological Survey of Canada (1994): Magnetic residual total field, Interior Plateau of British Columbia; *Geological Survey of Canada*, Open File 2785, 19 Maps, 1:100 000 and 1:250 000 scale.

Gordee, S., Andrews, G.D.M., Simpson, K.A. and Russell, J.K. (2007): Subaqueous channel-confined volcanism within the Chilcotin Group, Bull Canyon Provincial Park (NTS 093B/03), south-central British Columbia; *in* Geological Fieldwork 2006, *BC Ministry of Energy, Mines and Petroleum Resources*, Paper 2007-1 and *Geoscience BC*, Report 2007-1, pages 285–290.

Kerr, D.E. and Giles, T.R. (1993): Surficial geology of the Chezacut map area (NTS 93C/8); *BC Ministry of Energy, Mines and Petroleum Resources*, Open File 1993-17, 1:50 000 scale.

Levson, V.M. and Giles, T.R. (1997): Quaternary geology and till geochemistry studies in the Nechako and Fraser plateaus, central British Columbia (NTS 93C/1, 8, 9, 10; F/2, 3, 7; 93L/16; 93M/1); *in* Interior Plateau Geoscience Project: Summary of Geological, Geochemical and Geophysical Studies, Diakow, L.J., Metcalfe, P. and Newell, J., Editors, *BC Ministry of Energy, Mines and Petroleum Resources*, Paper 1997-2, pages 121–145.

Massey, N.W.D., MacIntyre, D.G., Desjardins, P.J. and Cooney, R.T. (2005): Digital geology map of British Columbia:

whole province; *BC Ministry of Energy and Mines*, GeoFile 2005-1, 1:250 000 scale, URL <http://www.em.gov.bc.ca/Mining/Geolsurv/Publications/GeoFiles/Gf2005-1/toc.htm>.

Mathews, W.H. (1989): Neogene Chilcotin basalts in south-central British Columbia: geology, ages, and geomorphic history; *Canadian Journal of Earth Sciences*, Volume 26, pages 969–982.

Metcalfe, P., Richards, T.A., Villeneuve, M.E., White, J.M. and Hickson, C.J. (1997): Physical and chemical volcanology of the Eocene Mount Clisbako volcano, central British Columbia (93B/12, 13; 93C/9, 16); *in* Interior Plateau Geoscience Project: Summary of Geological, Geochemical and Geophysical Studies, Diakow, L.J., Metcalfe, P. and Newell, J., Editors, *BC Ministry of Energy, Mines and Petroleum Resources*, Paper 1997-2, pages 31–61.

Mihalynuk, M.G., Erdmer, P., Ghent, E.D., Cordey, F., Archibald, D.A., Friedman, R.M. and Johannson, G.G. (2004): Coherent French Range blueschist: subduction to exhumation in <2.5 m.y.?; *Geological Society of America*, Bulletin, Volume 116, pages 910–922.

Mihalynuk, M.G., Peat, C.R., Orovan, E.A., Terhune, K., Ferby, T. and McKeown, M.A. (2008): Chezacut area geology (NTS 93C/8); *BC Ministry of Energy, Mines and Petroleum Resources*, Open File 2008-2, 1:50 000 scale.

MINFILE (2007): MINFILE BC mineral deposits database; *BC Ministry of Energy, Mines and Petroleum Resources,* URL <http://www.em.gov.bc.ca/Mining/Geolsurv/Minfile/> [November 2007].

Nebocat, J. (1983): Geological and geochemical report on the Chili claim; *BC Ministry of Energy, Mines and Petroleum Resources*, Assessment Report 11 685, 48 pages.

Parrish, R.R. (1983): Cenozoic thermal evolution and tectonics of the Coast Mountains of British Columbia: 1, Fission track dating, apparent uplift rates, and patterns of uplift; *Tectonics*, Volume 2, pages 601–631.

Peat, C., Mihalynuk, M.G., Ferbey, T. and Diakow, L.J. (2008): Analytical results from investigations in the Chezacut map area (NTS 93C/08) and other select areas within the Beetle Infested Zone 2007; *BC Ministry of Energy, Mines and Petroleum Resources*, GeoFile 2008-2.

Pynn, L. (2007): Quakes near Quesnel may signal lava flow; *The Vancouver Sun*, October 16, 2007.

Ray, G.E. (1995): Pb-Zn Skarns; *in* Selected British Columbia Mineral Deposit Profiles, Volume 1 — Metallics and Coal, Lefebure, D.V. and Ray, G.E., Editors, *BC Ministry of Energy of Employment and Investment*, Open File 1995-20, pages 61–62.

Ricketts, B.D., Evenchick, C.A., Anderson, R.G. and Murphy, D.C. (1992): Bowser Basin, northern British Columbia; constraints on the timing of initial subsidence and Stikinia – North America terrane interactions; *Geological Society of America,* Geology, Volume 20, pages 1119–1122.

Riddell, J.M. (2006): Geology of the southern Nechako Basin (NTS 92N, 92O, 93C, 93F, 93G), sheet 3 of 3 — geology with contoured gravity underlay; *BC Ministry of Energy, Mines and Petroleum Resources*, Petroleum Geology Map 2006-1, 1:400 000 scale.

Riddell, J.M., Ferri, F., Sweet, A.R. and O'Sullivan, P.B. (2007): New geoscience data from the Nechako Basin project; *in* The Nechako Initiative — Geoscience Update 2007, *BC Ministry of Energy, Mines and Petroleum Resources*, Petroleum Geology Open File 2007-1, pages 59–98.

Souther, J.G. and Souther, M.E.K. (1994): Geology, Ilgachuz Range and adjacent parts of the Interior Plateau, British Columbia; *Geological Survey of Canada*, Map 1845A, 1:50 000 scale.

Stout, M.Z. and Nicholls, J. (1983): Origin of the hawaiites from the Itcha Mountain Range, British Columbia; *Canadian Mineralogist*, Volume 21, pages 575–581.

Tipper, H.W. (1959): Geology, Quesnel; *Geological Survey of Canada*, Map 12-1959, 1:253 440 scale.

Tipper, H.W. (1969): Geology, Anahim Lake; *Geological Survey of Canada*, Map 1202A, 1:253 440 scale.

Tipper, H.W. (1971): Surficial geology, Anahim Lake; *Geological Survey of Canada*, Map 1289A, 1:250 000 scale.

Umhoefer, P.J. and Schiarizza, P. (1996): Latest Cretaceous to early Tertiary dextral strike-slip faulting on the southeastern Yalakom fault system, southeastern Coast Belt, British Columbia; *Geological Society of America Bulletin*, Volume 108, pages 768–785.

Yi, W., Halliday, A.N., Alt, J.C., Lee, D-C., Rehkämper, M., Garcia, M.O. and Su, Y. (2000): Cadmium, indium, tin, tellurium and sulfur in oceanic basalts: implications for chalcophile element fractionation in the Earth; *Journal of Geophysical Research – Solid Earth*, Volume 105, pages 18 927–18 948.